



HAL
open science

Sharp contrast in lithospheric structure across the Sorgenfrei Tornquist Zone as inferred by Rayleigh wave analysis of TOR1 project data

Nathalie Cotte, Helle Anette Pedersen

► **To cite this version:**

Nathalie Cotte, Helle Anette Pedersen. Sharp contrast in lithospheric structure across the Sorgenfrei Tornquist Zone as inferred by Rayleigh wave analysis of TOR1 project data. *Tectonophysics*, 2002, 360 (1-4), pp.75-88. 10.1016/S0040-1951(02)00348-7 . insu-03607063

HAL Id: insu-03607063

<https://hal-insu.archives-ouvertes.fr/insu-03607063>

Submitted on 8 May 2023

HAL is a multi-disciplinary open access archive for the deposit and dissemination of scientific research documents, whether they are published or not. The documents may come from teaching and research institutions in France or abroad, or from public or private research centers.

L'archive ouverte pluridisciplinaire **HAL**, est destinée au dépôt et à la diffusion de documents scientifiques de niveau recherche, publiés ou non, émanant des établissements d'enseignement et de recherche français ou étrangers, des laboratoires publics ou privés.



Distributed under a Creative Commons Attribution - NonCommercial| 4.0 International License

Sharp contrast in lithospheric structure across the Sorgenfrei–Tornquist Zone as inferred by Rayleigh wave analysis of TOR1 project data

N. Cotte, H.A. Pedersen*, TOR Working Group¹

Laboratoire de Géophysique Interne et Tectonophysique, Université Joseph Fourier, BP 53X, 38041, Grenoble Cedex 9, France

This work is a part of the TOR1 project (1996–1997) and is devoted to determining the lithospheric structure across the Sorgenfrei–Tornquist Zone in Northern Europe. For the first time in Europe, a very dense seismic broadband array has offered the possibility of determining very sharp lateral variations in the structure of the lithosphere at small scales using surface wave analysis. We measure phase velocities for Rayleigh waves with periods ranging between 10 and 100 s, both within arrays with apertures of 40–50 km (small compared to the wavelength), and along long profiles of at least 100 km. Dispersion curves are then inverted and shear-wave velocity models down to the depth of 200 km are proposed. We show that the Sorgenfrei–Tornquist Zone is a major tectonic feature within the whole lithosphere. North–east of this feature, in Sweden beneath the Baltic Shield, no lithosphere–asthenosphere boundary is observed to exist to depths of 200 km. South–west of the Sorgenfrei–Tornquist Zone, beneath Denmark, we find a lithospheric thickness of 120 ± 20 km. The transition across the Sorgenfrei–Tornquist Zone is sharp and determined to be very steeply dipping to the south–west. We also demonstrate the existence of a sharp discontinuity between the lithospheres beneath Denmark (120 ± 20 km thick) and beneath Germany (characterized by thicknesses of 50 ± 10 km in the northernmost part and 100 ± 20 km in the southwest). This discontinuity is most likely related to the Trans-European Fault at the surface.

Keywords: Lithospheric structure; Sorgenfrei–Tornquist Zone; Rayleigh wave analysis; TOR1 project data

* Corresponding author.

E-mail address: helle.pedersen@obs.ujf-grenoble.fr (H.A. Pedersen).

¹ TOR Working Group: S. Gregersen (coordinator), A. Berthelsen, H. Thybo, K. Mosegaard, T. Pedersen and P. Voss (Denmark); L.B. Pedersen, R.G. Roberts and H. Shomali (Sweden); R. Kind, G. Bock, J. Gossler, K. Wylegalla, W. Rabbel, I. Woelbern, M. Budweg, H. Busche, M. Korn and S. Hock (Germany); A. Guterch, M. Grad, M. Wilde-Piórko and M. Zuchniak (Poland); J. Plomerová (Czech Rep.); J. Ansorge, E. Kissling, R. Arlitt, F. Waldhauser and P. Ziegler (Switzerland); U. Achauer, H.A. Pedersen and N. Cotte (France); H. Paulssen (The Netherlands); E.R. Engdahl (USA).

1. Introduction

All previous studies (see below) agree in proposing significant lateral variations in the structure of the lithosphere across the Tornquist Zone. The Sorgenfrei–Tornquist Zone (STZ) divides Central Europe (Phanerozoic) from Fennoscandia (Proterozoic), whereas Central Europe and Eastern Europe are separated by the Teysseire–Tornquist Zone (TTZ). These two branches of the Tornquist Zone join between Germany and Sweden (e.g., Berthelsen, 1992; Guterch et al., 1986, 1994).

The STZ is the north-eastern border of the Tornquist Fan. This region is delimited to the south–west by the Trans-European Fault (TEF) (e.g., Berthelsen, 1992) and includes Denmark. The Tornquist Fan has an ambiguous origin: on the one hand, the STZ marks a sharp transition in the tectonic properties of the crust from the Baltic Shield (35–45 km thick) to the Tornquist Fan (≈ 32 km) (e.g., Tryggvason et al., 1998); on the other hand, however, the basement of the Tornquist Fan is similar to that of the Baltic Shield (e.g., Berthelsen, 1992). Compounding the ambiguity is the fact that lateral variations in the structure of the lithosphere are not as well constrained as crustal ones, as no dense, passive seismic experiment have been carried out in the area. Crustal models have been determined by reflection and refraction seismic studies such as FENNO-LORA (Guggisberg and Berthelsen, 1987), European GeoTraverse (1992), EUGENO-S Working Group (1988) and BABEL, and are well reported in the literature (Guggisberg et al., 1991; Thybo, 1990; Berthelsen, 1992; BABEL Working Group, 1993; Tryggvason et al., 1998; Thybo et al., 1998).

It is now well known that strong lateral variations exist in the lithosphere between the “old” Eastern Europe and the “young” Central Europe. Several surface wave studies have focused on this structure. Snieder (1988) determined a very sharp transition in lithospheric structure from one side of the TTZ to the other, between the depths of 100 and 200 km. Zielhuis and Nolet (1994) determined the seismic structure of the TTZ to a depth of at least 140 km, below which the contrast in velocity from a side to the other of the TTZ is smaller. Subsequently, Marquering and Snieder (1996) showed the existence of large lateral variations in lithospheric structure in the vicinity of the TTZ between the depths of

80 and 140 km, representing a sharp transition. Alsina and Snieder (1996) determined the direction of incident surface waves on the TTZ and showed that large lateral refractions occur on this zone. Using body waves, Schweitzer (1995) showed how the TTZ presents a blockage for P_n and P_g rays perpendicular to it. His observation of shadow areas leads to the proposal of a LVZ extending to a depth of 200 km. There is therefore no doubt that the TTZ is a major discontinuity down to depths of at least 200 km.

North of the TTZ, several studies have provided information about the thickness of the Baltic Shield and showed how it varies from one side of the STZ to the other. Using P-wave residuals, Husebye and Ringdal (1978) and Husebye and Hovland (1982) demonstrated that the Baltic Shield was characterized by high velocities down to depths of 250–300 km. From P- and S-wave refraction, Sacks et al. (1979) determined a Baltic Shield thickness of 250 ± 15 km at $2-3^\circ$ from the NORSAR array. In 1990, Dost showed that the lithosphere–asthenosphere boundary does not appear beneath the Baltic Shield. Using the fundamental and first two higher modes of Rayleigh waves, Calcagnile (1991) determined a LVZ extending between 140 and 350 km depth beneath Sweden, and between 220 and 290 km depth under the Baltic Sea. In 1994, Pedersen et al. employed an analysis of Rayleigh waves to determine that such a LVZ does not appear beneath Norway but exists beneath Denmark, between the depths of 120 and 220 km. Finally, by correlating lithospheric thicknesses with heat flux, Pollack and Chapman (1997) argued for the existence of a 200-km thick shield.

All these studies, except the one of Calcagnile (1991), agree in proposing a thick lithosphere for the Baltic Shield although disagreements remain with respect to the inferred value of the thickness and shear-wave velocities. In the south, the transition is expected to be sharp across the TTZ, while the sharpness is more disputed in the north across the STZ, especially because rocks of Proterozoic age have been found south–west of the STZ, and no seismic data on the area have had sufficient resolution to study the STZ on a lithospheric scale. This present study is thus devoted to the determination of the lithospheric structures across the STZ and the TEF.

2. The TOR1 seismic experiment and broad-band data

The TOR1 experiment (“Teleseismic TOMography Experiment across the TORnquist Zone”) took place in 1996–1997 with the goal of inferring the structure of the lithosphere across the Tornquist Zone by using tomography, receiver-function, anisotropy and surface wave studies (Gregersen et al., 1999). It represented a multinational effort (the participating countries and workers are listed at the beginning of the paper) and was part of EUROPROBE program.

One hundred twenty seismometers were installed from Göttingen (Germany) to Stockholm (Sweden) during the period covering September 1996 to May 1997. The location of the seismic stations is shown in Fig. 1 (modified after Gregersen et al., 1999). Among the seismic stations, 38 were broadband stations either from permanent networks or from the temporary experiment, which records are used for studying surface waves.

Six mini-arrays composed of three broadband stations are defined, some on each side of the STZ: two in Sweden (named S1 and S2), two in Denmark

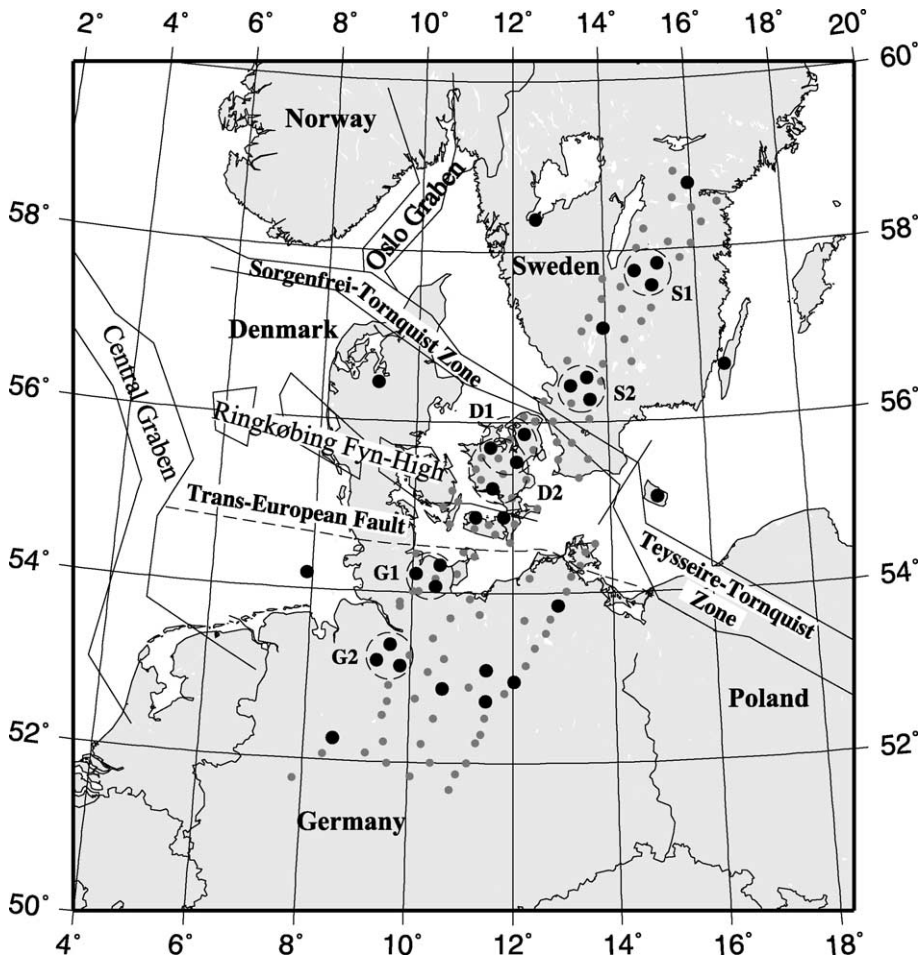


Fig. 1. Location of the short period stations (small grey points) and broadband stations (large black points) operating during the TOR1 experiment, from September 1996 to May 1997 (modified after Gregersen et al., 1999). Dashed circles represent the mini-arrays we used in this study.

(D1 and D2) and two in Germany (G1 and G2) (see Fig. 1). The stations are installed in triangles of 40–50 km width. The positioning of the mini-arrays permits the study of variations of lithospheric structure on the small scale of a few dozens of kilometers. Note that D2 and D1 arrays have two stations in common, but do not overlap in space. Phase velocities measured within these two arrays therefore correspond to different structures. One more array was available in Denmark, but could not be used due to GPS timing errors.

We selected 99 events for this study, with a magnitude greater than 5.1. The epicentral distance ranges from 15° to 155° and the azimuth coverage is very good, as shown in Fig. 2, as there is only a small gap between 310° and 345° . We discarded events for which the epicentral distance was larger than 155° to avoid problems due to multipathing and focusing/defocusing effects which can occur when

the source is close to the antipodes. Data were filtered between 5 and 200 s and corrected from the instrument response.

Fig. 3 shows 26 seismograms recorded on the vertical component by temporary and permanent broadband stations for a source located in the Atlantic ocean. The incident surface waves thus arrive from the south–west. The seismograms are all sorted by epicentral distance and the amplitude scale is the same for all of them. The first phase, recorded approximately at 1100 s by the nearest station to the source and at 1200 s by the further one, is the direct shear-wave. The main phase in amplitude is the Rayleigh wave, between 1700 and 2200 s. We note the good signal-to-noise ratio and the good coherence between records. Unfortunately, the signal-to-noise ratio of the horizontal components does not allow us to consider Love waves in the analysis. This is due to the thickness of the

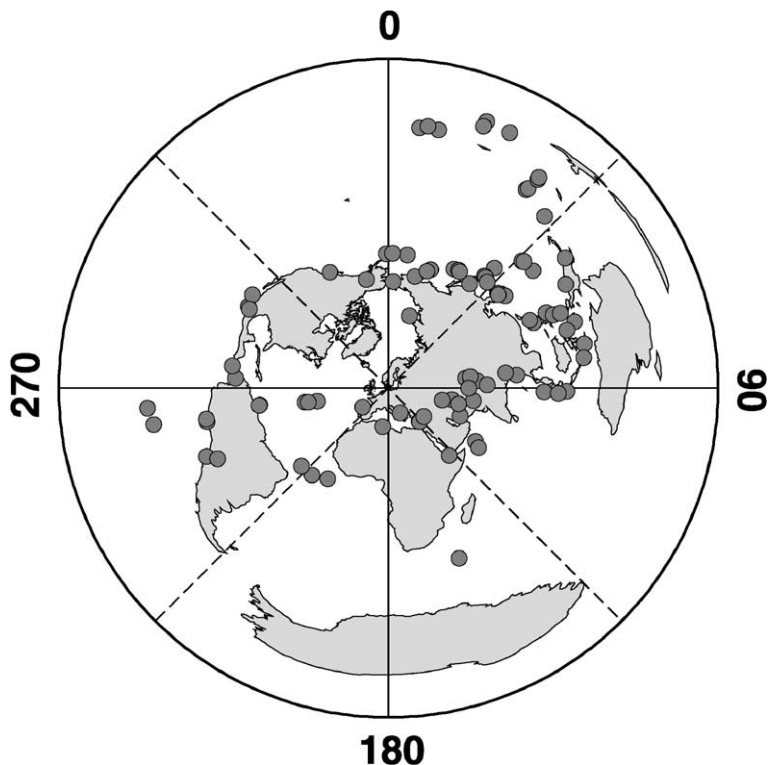


Fig. 2. Geographical distribution of the 99 events (grey dots) used in this study. The polar representation is centered in Denmark ($55^\circ\text{N}-12^\circ\text{E}$).

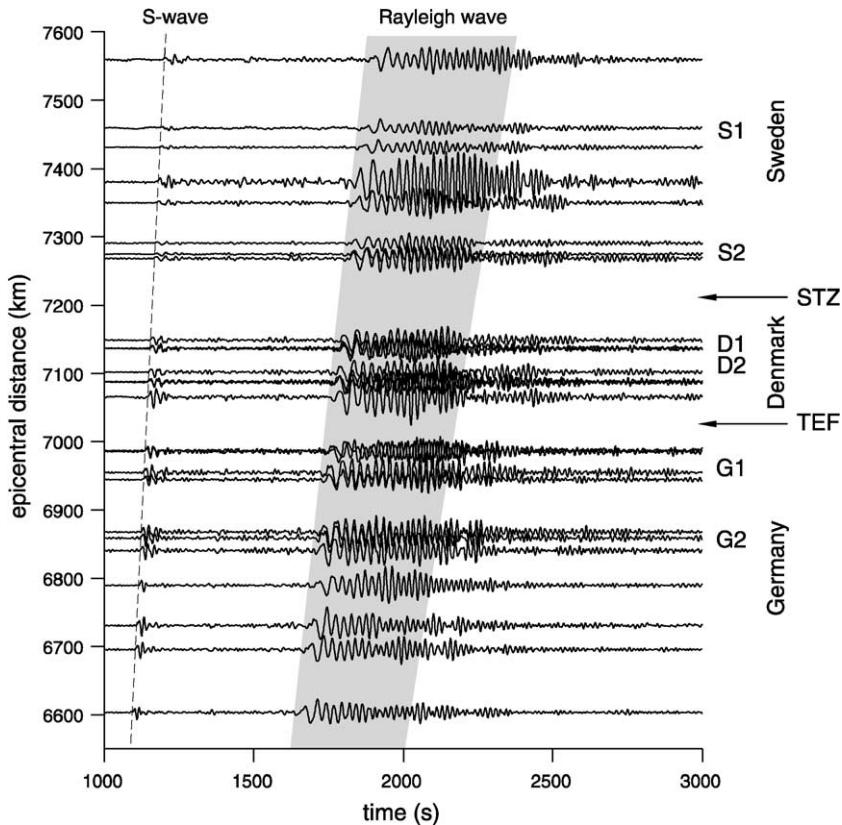


Fig. 3. Example of seismograms recorded on the vertical component by temporary and permanent broadband stations for the TOR1 experiment for an event located in the mid-Atlantic ridge (December 12, 1996). The seismograms are filtered between 5 and 200 s and corrected for instrument response. They are all sorted by epicentral distance and we use the same amplitude scale in all cases. The coherency between signals is high, so phase velocity measurements based on coherency can be performed.

sediments as well as noise from the sea affecting most of the stations.

3. Phase velocity measurements for Rayleigh waves

This section is devoted to phase velocity measurements of Rayleigh waves, both within mini-arrays and along long profiles of more than hundred kilometers. Within the mini-arrays, we used the method described by Cotte et al. (2000). In this paper, we presented the way to measure the phase velocity within arrays whose size is small compared to the wavelength of the surface waves. This analysis is possible thanks to the high coherence between stations. Firstly, we measure the arrival direction of the incident wave. For each frequency, we measure the time delay for all

the pairs of stations using the phase of the cross-spectrum. Knowing the distances between stations, the time delays are inverted to obtain the slowness vector. We directly get the arrival direction of the incident wave. Secondly, we report on a diagram the time delays as a function of the interstation distance corrected from the off-great circle deviation as determined by the slowness vector. Then, a linear regression through the points, and passing by the origin gives the phase velocity as the inverse of the slope of the line.

Large distances between stations are not necessary as long as the coherency between records is very high, so the phase velocity measurement within a small array is better adapted for studying laterally heterogeneous media than a measurement along a long profile, more than 100 km long, which neglects the

lateral heterogeneities. Measuring the phase velocity within a mini-array presents the advantage to take the observed off-great circle deviations into account. Cotte et al. (2000) showed that these deviations can reach up to 30° at 30 s period in the French Alps. It is however necessary to apply severe selection criteria to the data, and eliminate all records with an unstable phase. Nonetheless, for covering a large area of study we also measure the phase velocity along long profiles (several hundreds of kilometers). For this regional approach, we present phase velocities obtained along profiles averaged within each major tectonic unit.

Fig. 4a and b shows the dispersion curves measured for the Rayleigh wave in Denmark (D1 and D2

arrays) and Germany (G1 and G2 arrays), with respectively three, eight, four and five events. We did not succeed in measuring the phase velocities using the arrays located in Sweden because large amounts of data were missing, the data were very noisy, and the frequency band was too narrow for studying the lithospheric structure. The grey area is the confidence interval that we used in the inversion, determined by all our measurements. The black dots show the average value of the measured phase velocity.

In Fig. 4a, we can see that the phase velocity increases rapidly when the period varies from 20 to 35 s, and more slowly when the period varies from 35

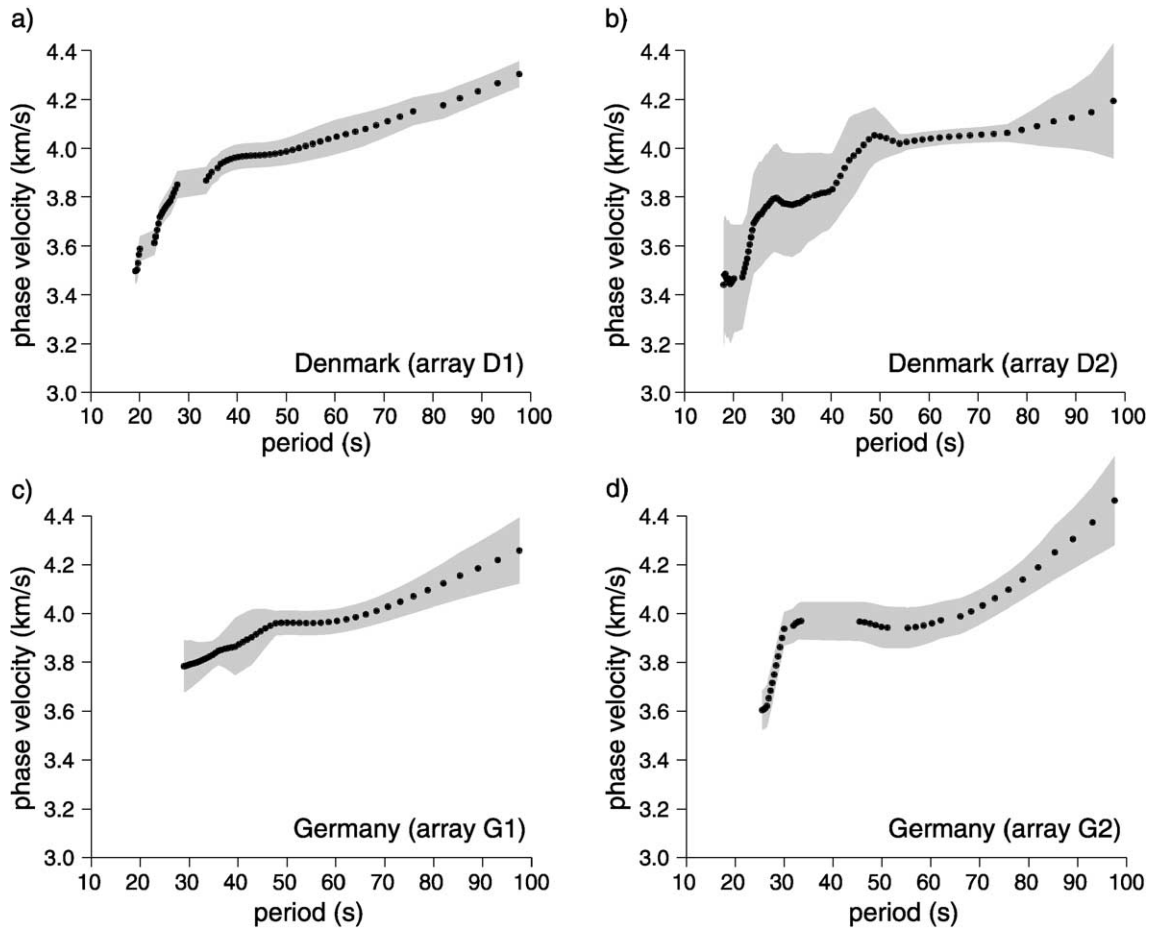


Fig. 4. Dispersion curves measured for the Rayleigh wave using the D1 and D2 arrays in Denmark (a and b) and the G1 and G2 arrays in Germany (c and d). The grey area is the confidence interval that we used in the inversion for determining lithospheric models. The black dots show the average value of the measured phase velocity.

to 100 s for the D1 array measurements. For the D2 array, a large scatter is observed in the measurements for periods shorter than 50 s and longer than 90 s. We thus decided to discard measurements lying outside 50–90 s. Within this frequency range, the phase velocity increases slightly with period and the confidence interval in velocity is small. For the G1 array (Fig. 4c), the phase velocity steadily increases when the period varies from 30 to 100 s. At 80–85 s period, the confidence interval is large, up to ± 1.5 km/s. Finally, the G2 array presents an important increase of the velocity when the period varies from 25 to 30 s, a constant velocity when the period varies from 30 to 70

s, and an increasing velocity for greater periods, reaching 4.4 km/s at 100 s period.

We also measured the phase velocity along profiles for which the interstation distance was greater than the wavelength at 30 s period, i.e. 100–120 km, using the Wiener filtering method (Wiener, 1949; see also Nakanishi, 1979; Taylor and Toksöz, 1982; Hwang and Mitchell, 1986). Fig. 5 shows all the profiles we used. We divided the area into three different zones which correspond to three tectonic units: Sweden (Baltic Shield, dark grey profiles), Denmark (between STZ and TEF, black profiles), and Germany (Phanerozoic Europe, light grey profiles). We respectively

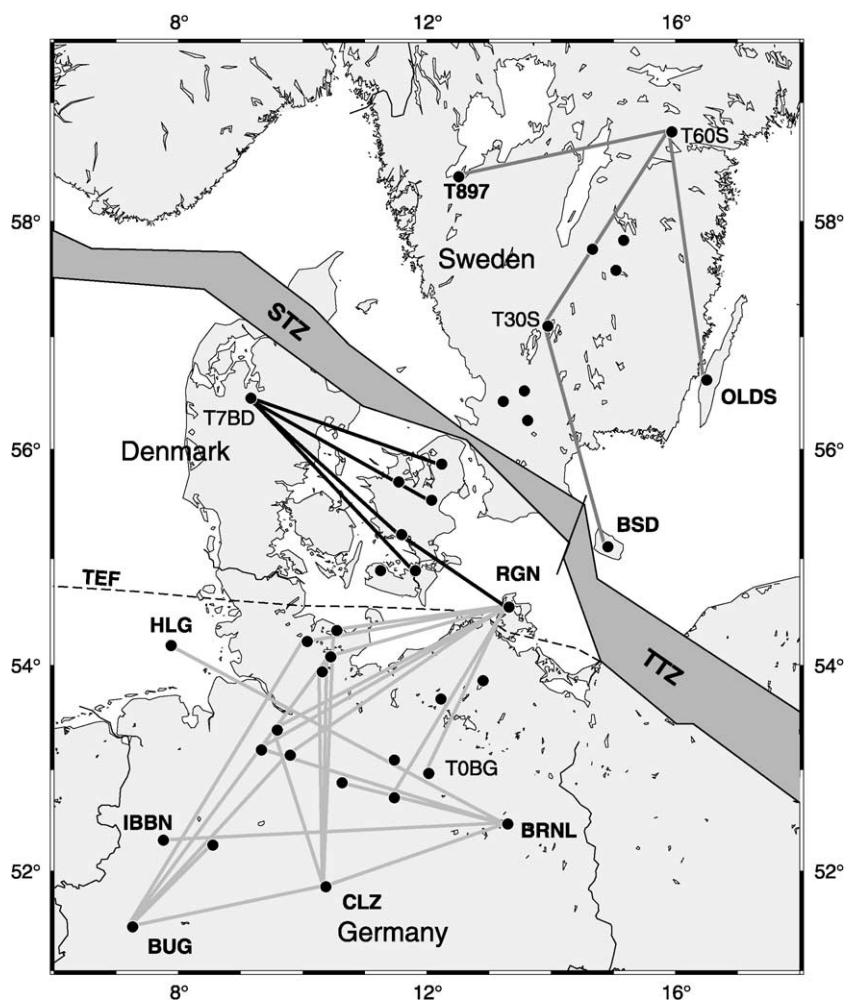


Fig. 5. Profiles of broadband stations used for measuring the phase velocity in Sweden (dark grey profiles), Denmark (black profiles), and Germany (light grey profiles) which correspond to three different tectonic areas.

made 9, 11 and 47 measurements along profiles, using 7, 6 and 28 different events, some of the measurements corresponding to a same event, but events are always selected so that the theoretical path and the station pairs present a misalignment lower than 5° . This precaution is for minimizing the effect due to off-great circle propagation as we can not correct the phase velocity of the great-circle deviation. We also verified that events from different directions yield approximately the same dispersion curves.

Results of phase velocity measurement along profiles are shown in Fig. 6. We can see in the shape of the dispersion curves that lithospheric models for the three areas must be different. For short periods, the

phase velocity is low in Germany (3.45 km/s at 20 s) as compared to Denmark and Sweden (3.65 and 3.60 km/s at 20 s). For intermediate periods (30–50 s), Denmark and Germany have same phase velocities, while they are up to 0.2 km/s larger for Sweden. Finally, for periods greater than 70 s, Sweden is characterized by larger phase velocity values (up to 4.5 km/s at 90 s) than Germany or Denmark (4.15 and 4.05 km/s). The dispersion curves within the arrays are different to the ones along the long profiles. The reason is that long profiles average the structure between the stations, while within a small array it is more obvious to work on a 1D model, assuming that the lateral heterogeneities of wavelength of 50–300

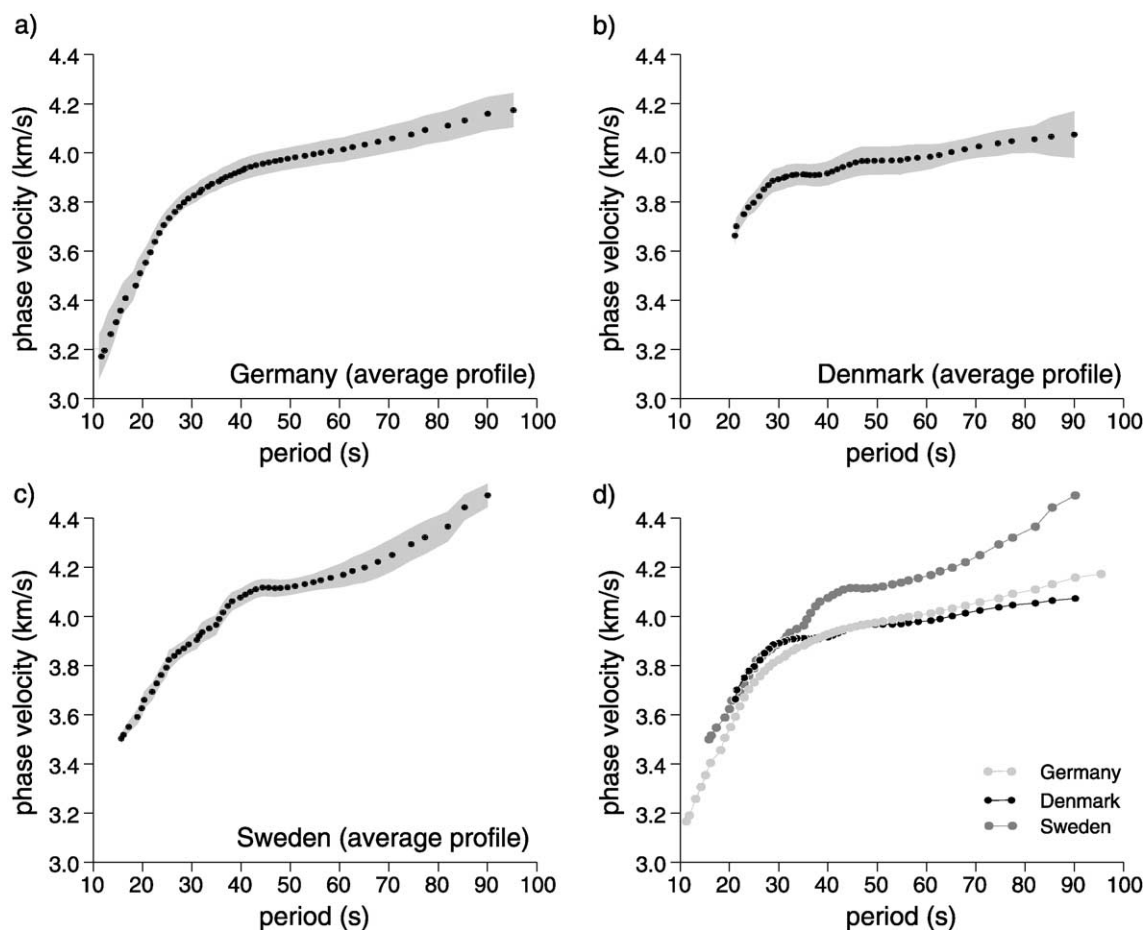


Fig. 6. Dispersion curves measured for Rayleigh waves along long profiles in Germany (a), Denmark (b) and Sweden (c). These three dispersion curves are superimposed on graph (d). The grey area is the confidence interval that we used in the inversion for determining lithospheric models. The black dots show the average values of the measured phase velocity.

km are large compared to the array aperture (40–50 km). Therefore, measurements along long profiles and within arrays must be inverted separately and will give complementary information on the lithospheric structures.

4. Inversion of dispersion curves: construction of lithospheric models

Using the seven dispersion curves of Figs. 4 and 6, we performed inversions to determine the corresponding lithospheric models in shear-wave velocity. We used the two-step method suggested by Shapiro et al. (1997). The first step consists in using a linearized inversion scheme as the one of Herrmann (1987). We get a simple lithospheric model, which is obtained by a root mean square fitting of the phase velocity dispersion curve. From this model, the second step consists in applying a random change either in velocity or in thickness for all the different layers. If the new model has a theoretical dispersion curve, which falls within our confidence interval, then the model is kept as a new solution and a new change is applied to it. Otherwise, we reconsider the last solution and apply a new change. This Monte-Carlo method allows us to explore the solutions for describing the set of possible models for which the dispersion curve fits within our confidence interval. By testing thousands of different models, we finally get a large set of solutions. The advantage is that we can explore all possible solutions and therefore avoid selecting a model corresponding to a secondary minimum in the inversion. We allow changes in the model to be up to 0.2 km/s in velocity for each layer, and of a few kilometers for the interface depth (the deeper is the interface, the bigger can be the change). We only accepted models for which crustal thicknesses and uppermost mantle velocities were coherent with results from refraction and/or reflection seismic profiling (e.g. Gregersen et al., 1993; Tryggvason et al., 1998; Thybo et al., 1998; Pedersen et al., 1999). The limits imposed were for crustal thicknesses 38 ± 2 km (Sweden), 32 ± 2 km (Denmark) and 30 ± 2 km (Germany). The imposed upper mantle velocities were 4.50–4.80 km/s (Sweden), 4.50–4.70 km/s (Denmark) and 4.40–4.70 km/s

(Sweden). Below this layer, no conditions are imposed on the S-wave velocities.

Fig. 7 shows in grey lines all the set of models found by inversion for the arrays. They are shear-wave velocity models expressed as a function of the depth and are reliable to depths of 200 km. For greater depths, we do not have the necessary resolution that would allow us to constrain the models. For all depths, we determine both the mean velocity as the average for all the possible models (solid line) and the mean using the minimal and maximal velocities (dashed line) to show the values given by ‘extreme’ models. The mean model is not one particular solution of the inversion. We determine the velocity in the uppermost mantle as the mean value found within the first kilometers beneath the Moho. The velocity at the minimum in the asthenosphere is the smallest value found by averaging all the models. Determining the lithospheric thickness is less obvious as there is a great variability in the models. We defined the minimum lithospheric thickness as the depth below which two-thirds of the models have an inverse gradient and the maximum lithospheric thickness as the depth where the velocity equals the minimum velocity of the asthenosphere +10% of its standard deviation. The average lithospheric thickness is determined as the average of these two values. We emphasize that having a rather smooth mean model makes the determination of the lithospheric thickness somewhat difficult, but this is a problem of real earth structure and not of the inversion procedure.

In Fig. 7, we can see that beneath the G1 and G2 arrays, the lithosphere–asthenosphere boundary is inferred to be at depths of 50 ± 10 and 75 ± 25 km, respectively. Shear-wave velocities in the upper mantle are respectively 4.43 ± 0.06 and 4.57 ± 0.08 km/s, and are 4.39 ± 0.05 and 4.36 ± 0.09 km/s at the minimum in the asthenosphere. For the G1 array, the large difference between the mean velocity (4.43 ± 0.06 km/s) in the uppermost mantle and the value given by the two extreme models (4.54 ± 0.16 km/s) shows that this velocity is not well determined. Beneath the D1 array, no lithosphere–asthenosphere boundary appears as the shear-wave velocity steadily increases with depth, to depths of at least 200 km. As the incident Rayleigh waves all arrive from north–east, we cannot exclude the possibility of a signature of the propagation in Sweden strongly affecting what

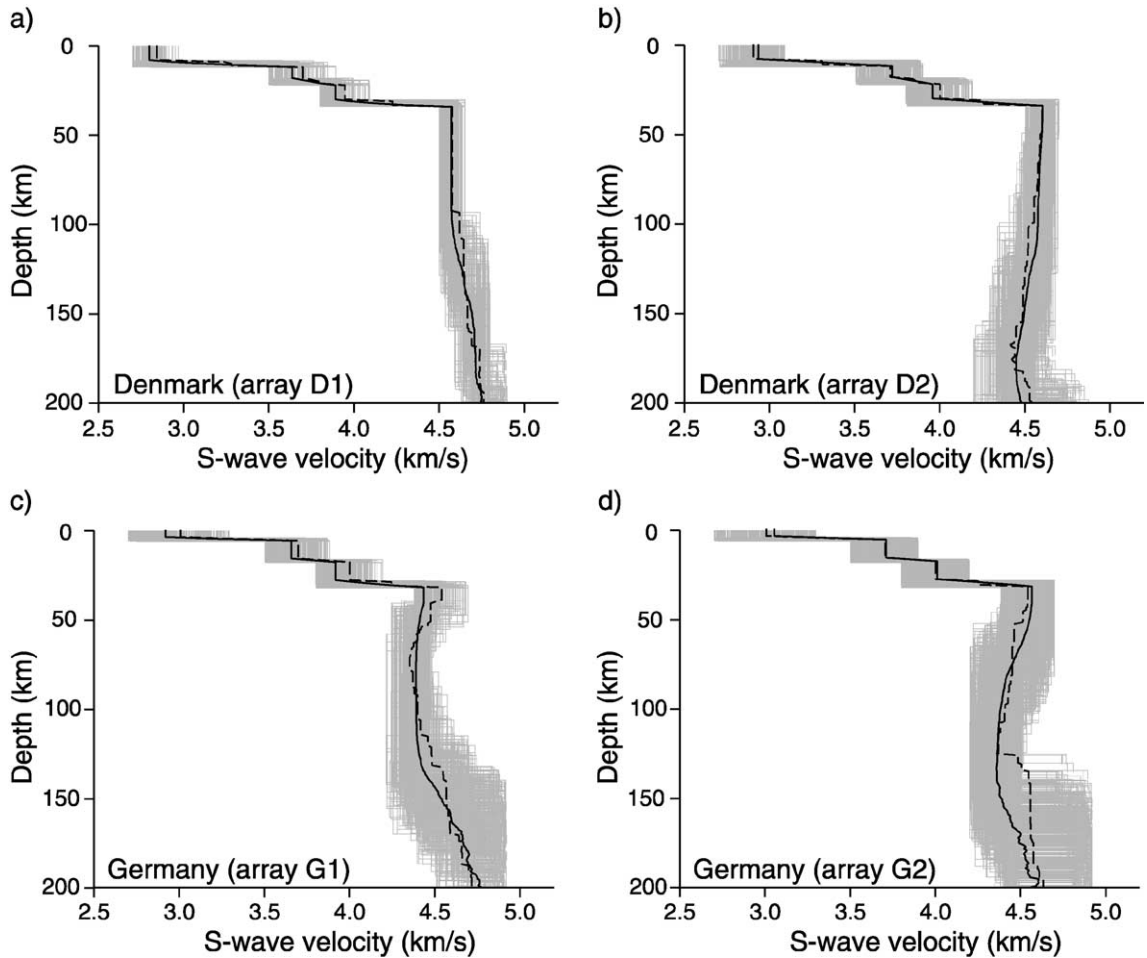
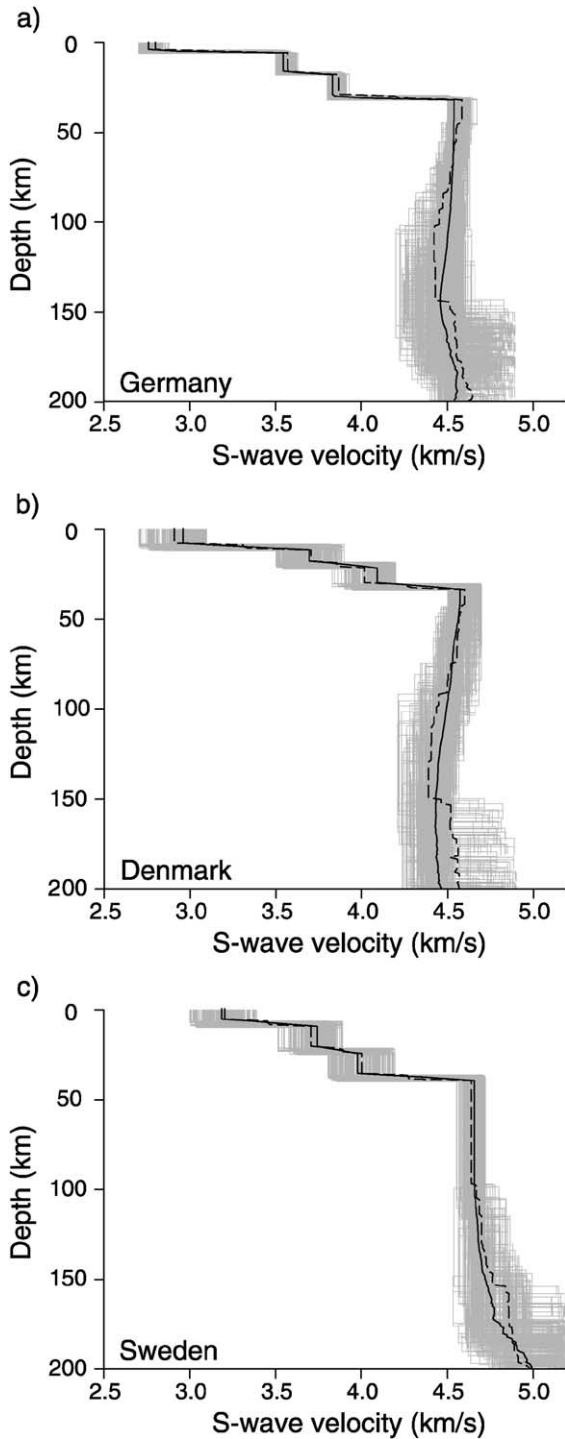


Fig. 7. Lithospheric models determined by inversion of the Rayleigh wave dispersion curves for the D1 and D2 arrays in Denmark (a and b) and the G1 and G2 arrays in Germany (c and d). Grey lines show all the models solution of the inversion, while solid black line gives the mean velocity over all models and the dashed black line is the average between the minimal and maximal velocities.

we determine within the D1 array. Fifty kilometers to the south–west of this array, beneath the D2 array, we determine a lithosphere–asthenosphere boundary located at the depth of 120 ± 20 km, with shear-wave velocity of 4.60 ± 0.04 km/s in the upper mantle and 4.45 ± 0.09 km/s at the minimum in the asthenosphere.

The same inversion procedure was used for the dispersion curves measured along profiles in Germany, Denmark, and Sweden (see Fig. 6). Results for these three areas are presented in Fig. 8. Beneath Germany (Fig. 8a), the lithosphere is rather thin with an average thickness of 100 ± 20 km, and shear-wave

velocities of 4.54 ± 0.03 and 4.46 ± 0.08 km/s in the upper mantle and at the minimum in the asthenosphere, respectively. The lithospheric structure determined along long profiles is thicker than the one determined beneath the G1 and G2 arrays, but profiles cover a much greater area than the two arrays. Surprisingly, the velocity at the minimum in the asthenosphere is larger using all profiles than the ones found beneath the two arrays. We speculate that this is due to the fact that the velocity is determined as a greater depth as compared to the arrays, which might be correlated to the thicker lithosphere. Beneath Denmark (Fig. 8b), the lithosphere is 120 ± 20 km thick



and the shear-wave velocities are almost the same as in Germany: 4.57 ± 0.06 km/s in the upper mantle and 4.43 ± 0.08 km/s at the minimum in the asthenosphere. In that case, the lithosphere thickness and velocities are the same as the ones determined beneath the D2 array. This may indicate that no large lateral heterogeneities are likely to exist beneath Denmark, apart from the variation between D1 and D2. Finally, we show the inversion for measurements along profiles in Sweden (Fig. 8c). This model does not present any lithosphere–asthenosphere boundary to depth of at least 200 km. No array analysis was available for this area. The shear-wave velocity determined in the upper mantle, of 4.66 ± 0.03 km/s, is higher than the ones determined for Denmark or Germany.

5. Discussion and conclusion

In Table 1, we have summarized our results for the thicknesses of the lithosphere and the shear-wave velocities in the upper mantle that we determined under Sweden, Denmark and Germany by the inversion of Rayleigh wave dispersion curves. We propose in Fig. 9 a lithospheric model along the TOR1 profile. This model is constructed using the results from the four arrays, and outside them using the available information from the three average models from Sweden, Denmark and Germany.

North of the Sorgenfrei–Tornquist Zone, beneath the Baltic Shield in Sweden, no lithosphere–asthenosphere boundary is inferred to depths of at least 200 km. Our results are consistent with the ones of Husebye and Ringdal (1978), Stuart (1978), Husebye and Hovland (1982), Sacks et al. (1979), Dost (1990), Pedersen et al. (1994) and Pollack and Chapman (1997). They are consistent with the result of Calcagnile (1982, 1991) for the Danish area, but in disagreement on the structure beneath southern Sweden. However, due to a poor station coverage of the area prior the TOR experiment, direct comparison between their studies and ours is somewhat difficult. We also have no lithosphere–asthenosphere boundary appearing under the D1 array located just south–west of the

Fig. 8. Lithospheric models determined by inversion of the Rayleigh wave dispersion curves under Germany (a), Denmark (b) and Sweden (c).

Table 1

Lithospheric thickness (Z) in km and shear-wave velocities in the upper mantle (V_{S0}) and at the minimum in the asthenosphere (V_{S1}), in km/s, as determined by the inversion of Rayleigh wave dispersion curve

Area	Z	V_{S0}	V_{S1}
S	>200	4.66 ± 0.03	
D1	>200	4.57 ± 0.04	
D2	120 ± 20	4.60 ± 0.04	4.45 ± 0.09
D	120 ± 20	4.57 ± 0.06	4.43 ± 0.08
G1	50 ± 10	4.43 ± 0.06	4.39 ± 0.05
G2	75 ± 25	4.57 ± 0.08	4.36 ± 0.09
G	100 ± 20	4.54 ± 0.03	4.46 ± 0.08

See text for details. Bold letters are for long aperture profiles located in the three different countries (Sweden, Denmark and Germany) and the others are the arrays (D1, D2, G1 and G2).

Sorgenfrei–Tornquist Zone. Beneath Denmark, with the exception of the structure determined under the D1 array, the lithospheric thickness is 120 ± 20 km. We observed no lateral variations in the depth of the lithosphere–asthenosphere boundary and only small variations for the shear–wave velocities in the upper mantle and at the minimum in the asthenosphere. Finally, beneath Germany we determined a very thin lithosphere of thickness smaller or equal to 100 ± 20 km, in particular close to Denmark where the G1 and G2 arrays are located.

We thus conclude that the major discontinuity in the lithospheric structure across the Tornquist Fan is located between Denmark and Sweden, where the Sorgenfrei–Tornquist Zone lies at the surface. Indeed, within a few dozens of kilometers the lithospheric

structure changes laterally very rapidly and the Sorgenfrei–Tornquist Zone is confirmed to be a major tectonic feature to depths of at least 200 km. As we have the same lithospheric structure beneath Sweden and beneath the D1 array located in Denmark, just south–west to the Sorgenfrei–Tornquist Zone, we conclude that the tectonic transition is sharp, dipping steeply to the south–west. The Baltic Shield extends under the D1 array, but does not appear under the D2 array, which is 50 km further from the STZ.

A second and smaller discontinuity is also determined across the Trans-European Fault located between Denmark and Germany, south of the Ringkbing Fyn High (Fig. 1). North of it, in Denmark, the lithosphere is 120 ± 20 km thick and the shear-wave velocity at the minimum in the asthenosphere is approximately 4.43–4.45 km/s. South of it, in Germany, the thickness of the lithosphere is smaller, of 50 ± 10 km under the G1 array, and the shear-wave velocity inferred to be 4.39 km/s at the minimum in the asthenosphere beneath the G1 array is rather low. Even if the Trans-European fault is a postulated one (Berthelsen, 1984), our results show significant contrasts in the lithospheric structure across its assumed location.

The only other previous surface wave study that specifically addresses the STZ (Pedersen et al., 1994) showed a significant difference between Western Denmark and Eastern Norway. They determined a 120-km thick lithosphere beneath the former, and no lithosphere–asthenosphere boundary beneath the latter,

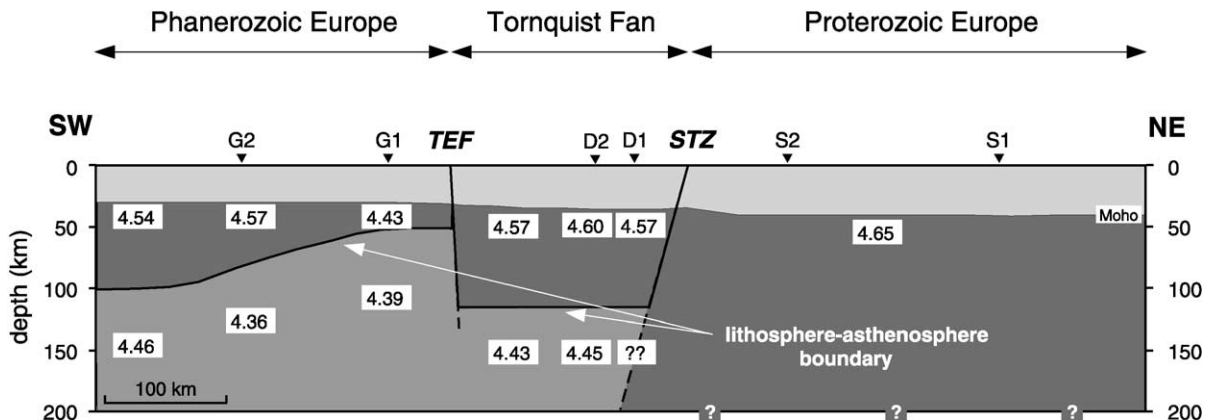


Fig. 9. Model of the lithosphere beneath the TOR1 profile, from Germany to Sweden through Denmark, based on the analysis of Rayleigh waves presented in the text. STZ = Sorgenfrei–Tornquist Zone. TEF = Trans-European Fault.

which is consistent with our results. We improved the constraint of lateral variation by having much more stations and by performing array analysis on a small scale as compared to the wavelength of the studied Rayleigh waves, thereby limiting the contrast in lithospheric structure to the STZ.

More recently, by performing P-wave tomography within the context of the TOR1 experiment, Arlitt et al. (2000) showed that no lithosphere–asthenosphere boundary exists beneath the Baltic Shield to a depth of 200 km and that the lithosphere is 120 km beneath Denmark but otherwise relatively thin (50 km) beneath Germany. Note that they did not have a good resolution at this depth due to the limit of the “crustal” model (50 km thick) used for the travel time inversion (Arlitt et al., 1999). Their results for the thickness of the lithosphere and the geometry of the tectonic feature beneath the Sorgenfrei–Tornquist Zone, dipping steeply to the south–west, are in good agreement with ours. On the other hand, Pedersen et al. (1999) found that this Zone presented a dipping steeply to the north–east, as a conclusion of their P-wave travel time residuals. Their results are then in contradiction with ours and the ones of Arlitt et al. (2000). However, we clearly find the same structure as this latter by using very different and independent methods applied to different phases of the signals recorded by the TOR1 experiment. As expected, the relative variations in velocities at the minimum in the asthenosphere are higher as we analyze shear-wave velocities, which are more sensitive to the partial melt. Accepting that the thickness and velocity models are now well constrained across the Sorgenfrei–Tornquist Zone, it becomes important to better understand the mechanisms that led to the juxtaposition of such different lithospheric structures.

Acknowledgements

NC thanks S. Gregersen for giving her the opportunity to go to Copenhagen and to participate in the fieldwork, and also for fruitful discussions and comments of this work. The authors are indebted to A. Paul for careful commenting a preliminary version of the manuscript, and to M. Grad and an anonymous reviewer for constructive reviews. NC was supported by a contract between the Centre National de la

Recherche Scientifique and the Laboratoire de Détection et de Géophysique, No. 72B 087/00.

This is a EUROPROBE publication.

References

- Alsina, D., Snieder, R., 1996. Constraints on the velocity structure beneath the Tornquist–Teisseyre Zone from beam-forming analysis. *Geophys. J. Int.* 126, 205–218.
- Arlitt, R., Kissling, E., Ansorge, J., TOR Working Group, 1999. 3-D crustal structure beneath the TOR array and effects on teleseismic wavefronts. *Tectonophysics* 314, 309–319.
- Arlitt, R., et al., TOR Working Group, 2000. P-wave velocity structure of the lithosphere–asthenosphere system across the TESZ in Denmark. Presented to the European Geophysical Society Meeting, Nice, France, April 2000. *EGS Newsletter*, vol. 74, p. 77.
- BABEL Working Group, 1993. Deep seismic reflection/refraction interpretation of crustal structure along BABEL profiles A and B in the southern Baltic Sea. *Geophys. J. Int.* 112, 325–343.
- Berthelsen, A., 1984. The early (800–300 Ma) crustal evolution of the off-shield region in Europe. In: Galson, D.A., Mueller, St. (Eds.), *First EGT Workshop, The Northern Segment*. European Science Foundation, Strasbourg, pp. 125–142.
- Berthelsen, A., 1992. Mobile Europe. In: Blundell, D., Freeman, R., Mueller, S. (Eds.), *The European Geotraverse: A Continent Revealed*. Cambridge Univ. Press, Cambridge, pp. 153–164.
- Calcagnile, G., 1982. The lithosphere–asthenosphere system in Fennoscandia. *Tectonophysics* 90, 19–35.
- Calcagnile, G., 1991. Deep structure of Fennoscandia from fundamental and higher mode dispersion of Rayleigh waves. *Tectonophysics* 195, 139–149.
- Cotte, N., Pedersen, H.A., Campillo, M., Farra, V., Cansi, Y., 2000. Off-great circle propagation of intermediate period surface waves as observed on a dense array in the French Alps. *Geophys. J. Int.* 142, 825–840.
- Dost, B., 1990. Upper mantle structure under western Europe from fundamental and higher mode surface waves using the NARS array. *Geophys. J. Int.* 100, 131–151.
- EUGENO-S Working Group, 1988. Crustal structure and tectonic evolution of the transition between the Baltic Shield and the North German Caledonides (the EUGENO-S Project). *Tectonophysics* 150, 253–348.
- European Geotraverse, 1992. In: Blundell, D., Freeman, R., Mueller, S. (Eds.), 1992. *The European Geotraverse: A Continent Revealed*. Cambridge Univ. Press, Cambridge.
- Gregersen, S., Thybo, H., Perčić, E., 1993. Interpretation from explosion seismograms of crustal inhomogeneities in Statu Nascendi. *Pol. Acad. Sci.* 255, 87–89.
- Gregersen, S., Tor Working Group, 1999. Important findings expected from Europe’s largest seismic array. *EOS Trans.* 80, 1–2.
- Guggisberg, B., Berthelsen, A., 1987. A two-dimensional velocity model for the lithosphere beneath the Baltic Shield and its possible tectonic significance. *Terra Cognita* 7, 631–637.
- Guggisberg, B., Kaminski, W., Prodehl, C., 1991. Crustal structure

- of the Fennoscandian Shield: a travelttime interpretation of the long-range FENNOLOGRA seismic refraction profile. *Tectonophysics* 195, 105–137.
- Guterch, A., Grad, M., Materzok, R., Perchuc, E., 1986. Deep structure of the earth's crust in the contact zone of the Paleozoic and Precambrian platforms in Poland (Tornquist–Teisseyre zone). *Tectonophysics* 128, 251–279.
- Guterch, A., Grad, M., Janik, T., Materzok, R., Luosto, U., Yliniemi, J., Lück, E., Schulze, A., Förste, K., 1994. Crustal structure of the transition zone between Precambrian and Variscan Europe from new seismic data along LT-7 profile (NW Poland and eastern Germany). *C. R. Acad. Sci. Paris* 319 II, 1489–1496.
- Herrmann, R.B., 1987. Computer programs in seismology. Saint Louis University.
- Husebye, E.S., Hovland, J., 1982. The upper mantle seismic heterogeneities beneath Fennoscandia. *Tectonophysics* 90, 1–17.
- Husebye, E.S., Ringdal, F., 1978. Seismic mapping of the Fennoscandian lithosphere and asthenosphere with special reference to the Oslo graben. In: Ramberg, I.B., Neumann, E.-R. (Eds.), *Tectonics and Geophysics of Continental Rifts*. Dordrecht, Holland, pp. 297–311.
- Hwang, H.J., Mitchell, B.J., 1986. Interstation surface wave analysis by frequency-domain Wiener deconvolution and modal isolation. *Bull. Seism. Soc. Am.* 76, 847–864.
- Marquering, H., Snieder, R., 1996. Shear-wave velocity structure beneath Europe, the northeastern Atlantic and western Asia from waveform inversion including surface-wave mode coupling. *Geophys. J. Int.* 127, 283–304.
- Nakanishi, I., 1979. Phase velocity and Q of mantle Rayleigh waves. *Geophys. J. R. Astron. Soc.* 58, 35–59.
- Pedersen, H.A., Campillo, M., Balling, N., 1994. Changes in the lithospheric structure across the Sorgenfrei–Tornquist Zone inferred from dispersion of Rayleigh waves. *Earth Planet. Sci. Lett.* 128, 37–46.
- Pedersen, T., Gregersen, S., Tor Working Group, 1999. Project TOR: deep lithospheric variation across the Sorgenfrei–Tornquist Zone, Southern Scandinavia. *Bull. Geol. Soc. Den.* 46, 13–24.
- Pollack, H.N., Chapman, D.S., 1997. On the regional variation of heat flow, geotherms and lithospheric thickness. *Tectonophysics* 38, 279–296.
- Sacks, I.S., Snoke, J.A., Husebye, E.S., 1979. Lithosphere thickness beneath the Baltic Shield. *Tectonophysics* 56, 101–110.
- Shapiro, N.M., Campillo, M., Paul, A., Singh, S.K., Jongmans, D., Sanchez-Sesma, F.J., 1997. Surface-wave propagation across the Mexican Volcanic Belt and the origin of the long-period seismic-wave amplification in the valley of Mexico. *Geophys. J. Int.* 128, 151–166.
- Schweitzer, J., 1995. Blockage of regional seismic waves by the Teisseyre–Tornquist zone. *Geophys. J. Int.* 123, 260–276.
- Snieder, R., 1988. Large-scale waveform inversions of surface waves for lateral heterogeneity: 2. Application to surface waves in Europe and the Mediterranean. *J. Geophys. Res.* 93, 12067–12080.
- Stuart, G.W., 1978. The upper mantle structure of the North Sea region from Rayleigh wave dispersion. *Geophys. J. R. Astron. Soc.* 52, 367–382.
- Taylor, S.R., Toksöz, M.N., 1982. Measurement of interstation phase and group velocities and Q using Wiener filtering. *Bull. Seism. Soc. Am.* 72, 73–91.
- Thybo, H., 1990. A seismic velocity model along the EGT profile from the North German Basin into the Baltic Shield. In: Freeman, R., Giese, P., Mueller, S. (Eds.), *The European Geotraverse: Integrative Studies*. European Science Foundation, Strasbourg, pp. 99–108.
- Thybo, H., Perchuc, E., Gregersen, S., 1998. Interpretation in statu nascendi of seismic wide-angle reflections based on EUGENOS data. *Tectonophysics* 289, 281–294.
- Tryggvason, A., Lund, C.-E., Friberg, M., 1998. A two-dimensional seismic velocity model across the transition zone between the Baltic Shield and the North German Basin—the EUGENOS profile 1 revisited. *Tectonophysics* 290, 47–58.
- Wiener, N., 1949. *Time Series*. MIT Press, Cambridge, MA, 163 pp.
- Zielhuis, A., Nolet, G., 1994. The deep seismic expression of an ancient plate boundary in Europe. *Science* 265, 79–81.